J Gen Plant Pathol (2006) 72:57–64
DOI 10.1007/s10327-005-0243-y

DISEASE CONTROL

**Abhinandan Deora · Yasuyuki Hashidoko
Md. Tofazzal Islam · Yuriko Aoyama · Toshiaki Ito
Satoshi Tahara**

An antagonistic rhizoplane bacterium *Pseudomonas* sp. strain EC-S101 physiologically stresses a spinach root rot pathogen *Aphanomyces cochlioides*

Received: January 5, 2005 / Accepted: July 15, 2005

Abstract We observed that an antagonistic rhizoplane bacterium *Pseudomonas* sp. strain EC-S101 induces excessive lateral and apical branching in the hyphae of a root rot phytopathogen *Aphanomyces cochlioides* AC-5 resulting in radial growth inhibition of hyphae in a dual culture assay. Confocal laser scanning microscopic observations using fluorescent stains indicated an increased quantity of nuclei and lipid bodies in the affected hyphae during the early stage (less affected hyphae) at day 3 of interaction. At a more advanced stage (severely affected hyphae) at day 3, nuclei became smaller and round-shaped compared with the oval shape in AC-5 control hyphae. After 7 days, nuclei disintegrated, and the nuclear materials were released into the disorganized cytoplasm. With transmission electron microscopy at 5 days of interaction, we found that the cell walls of AC-5 hyphae were considerably thicker than those of the control. Enlarged vacuoles, lipid bodies sunk into vacuoles, and vacuoles filled with electron-dense material, followed by an invagination of the AC-5 hyphal cell wall, were commonly observed. Nonmembranous electron-transparent inclusion bodies irregular in size were often distributed in the affected hyphae. By integrating our observations, we conclude that antagonistic effects evoked by strain EC-S101 resulted in the death of AC-5 hyphae, which might contribute to the suppression of *A. cochlioides* AC-5-linked damping-off disease in its host plants.

Key words Antagonistic rhizobacteria · Anti-Peronosporomycetes · Confocal laser scanning microscopic observation · Excessive branching · *Pseudomonas jessenii*

A. Deora · Y. Hashidoko (✉) · M.T. Islam · Y. Aoyama · T. Ito · S. Tahara
Graduate School of Agriculture, Hokkaido University, Kita-ku, Sapporo 060-8589, Japan
Tel. +81-11-706-3840; Fax +81-11-706-4182
e-mail: yasu-h@abs.agr.hokudai.ac.jp

The nucleotide sequence data reported are available in the DDBJ/EMBL/GenBank databases under the accession number AB190286

Introduction

Aphanomyces cochlioides, a soilborne phytopathogenic Peronosporomycete, causes root rot in spinach, sugar beet, and other members of Chenopodiaceae and Amaranthaceae. Numerous approaches for the biological control of this soilborne pathogen have used antagonistic bacteria that can suppress damping-off and other Peronosporomycetes *Pythium* and *Phytophthora* (Homma et al. 1993; Williams and Asher 1996; Dunne et al. 1998; Nakayama et al. 1999). Among the biocontrol agents, extensive research has been done with promising candidates in the genus *Pseudomonas* because of their potential to produce a diverse array of antifungal compounds that suppress soilborne pathogens during their interactions in the rhizosphere (Huang et al. 2004; Savchuk and Fernando 2004). While there have been a few studies on the detailed interactions between Peronosporomycete pathogens and *Pseudomonas* spp. (Bolwerk et al. 2003) or their metabolites (Thrane et al. 1999; Bolwerk et al. 2003), these have been limited among studies directed toward a better understanding of the biological control process.

In our previous work that emphasized the importance of microbe–microbe interactions in the context of biorational control of soilborne phytopathogens, we proposed that antagonistic prokaryotic rhizoplane bacteria induce morphological alterations in the hyphae of eukaryotic Peronosporomycetes in dual culture assays (Deora et al. 2005). Among the characterized antagonistic rhizoplane bacteria, *Pseudomonas* sp. strain EC-S101 induces excessive branching through apical bifurcation in *A. cochlioides* AC-5 hyphae resulting in radial growth inhibition in dual culture assay (Deora et al. 2005). In the same study, we showed that EC-S101 also suppressed in vitro damping-off disease in its host plants mediated by AC-5 (Deora et al. 2005). Prokaryotes and eukaryotes are ubiquitous cohabitants in myriads of environments, and they are capable of exhibiting both antagonistic and synergistic effects upon one another (Whipps 2001; Hogan and Kolter 2002). Therefore, to further our understanding of the morphological

abnormality induced in AC-5 hyphae and its possible contribution to disease suppression, we explored the physiological effects at the cellular level that are not visible under the light microscope.

Cellular changes in phytopathogens induced by fungicides and biocontrol agents have been studied extensively with transmission electron microscopy (TEM) to understand the mechanism of inhibition (Benhamou et al. 1999; Kang et al. 2001). Thrane et al. (1999) used vital fluorescent stains developed to study animal and human cell physiology to study the cellular responses in fungi to bacterial metabolites. These same fluorescent dyes were used by Hansen et al. (2000) with confocal laser scanning microscopy (CLSM) to precisely describe fungal responses to a bacterial antibiotic. However, to the best of our knowledge, no previous in vitro study has visualized and documented the dynamics of the physiological changes at the subcellular level in the hyphae of a soilborne eukaryotic phytopathogen during its interaction with an antagonistic prokaryote.

To elucidate the mode of action of EC-S101 against AC-5, we investigated the interactions between AC-5 mycelia and bacterial colonies of EC-S101 in a dual culture agar assay at the ultrastructural level using CLSM and TEM. Here we describe the physiological and subcellular changes associated with morphological abnormalities induced in *A. cochlioides* AC-5 when cultured with *Pseudomonas* sp. strain EC-S101, in relation to the behavior of specific cell organelles such as the nucleus, mitochondrion, lipid body, vacuole, and cell wall.

Materials and methods

Microorganisms

The bacterium *Pseudomonas* sp. strain EC-S101 was isolated from the rhizoplane of spinach (*Spinacia oleracea*) roots as described (Deora et al. 2005). The 16S RNA gene sequence of the EC-S101 has been deposited in the DNA Data Bank of Japan (DDBJ) under accession no. AB190286 and is tentatively identified as *Pseudomonas jessenii*. This bacterial isolate suppressed damping-off disease on sugar beet seedlings infected with *Aphanomyces cochlioides*. The pretreatment of sugar beet seeds with EC-S101 at 1×10^8 CFU (colony forming unit) per seed showed almost equivalent damping-off suppression to that treated with hymexazol, a conventional fungicide, at 7.5 g/kg seeds, when the seedlings grown from respective seeds and inoculated with 10^2–10^3 zoospores per seedlings in pots (Deora et al. 2005). Further tests on biochemical, morphological, and physiological features of the bacterium are in progress and will facilitate appropriate taxonomic determination. The test pathogen *A. cochlioides* AC-5 was kindly donated by Professor R. Yokosawa, Health Science University of Hokkaido, Japan. AC-5 was originally isolated by Professor R. Yokosawa from a sugar beet field affected in Hokkaido by damping-off disease.

Dual culture tests

Interactions between *A. cochlioides* AC-5 and *Pseudomonas* sp. strain EC-S101 were studied according to the following procedure. Agar discs (6 mm in diameter) were collected from the growing edges of AC-5 hyphae on corn meal agar (CMA, 17 g/l, Difco Laboratories, Sparks, MD, USA) and placed 3 cm from the colonies of bacterial strain EC-S101. Plates were allowed to grow at 27°C in the dark. For CLSM observations, AC-5 hyphal samples were harvested with a sterile cork borer (6 mm i.d.) from the colony edge growing toward the EC-S101 colonies after 3 days. For TEM observations, samples of AC-5 were similarly harvested after 5 days of coculture on potato dextrose agar (PDA) (potato dextrose broth, 24 g/l, Difco Laboratories; agar, 20 g/l) medium. Encircled areas in Fig. 1 indicate the parts of agar discs harvested by a sterile cork borer (6 mm i.d.) for CLSM and TEM study of AC-5 hyphae growing toward EC-S101 on PDA. When grown on PDA, the mycelial density of *A. cochlioides* was relatively higher in comparison with growth on CMA. As a result, to facilitate CLSM visualization, the pathogen and bacteria were grown on CMA at 27°C, while PDA was used for TEM. For comparisons, untreated negative controls were harvested from

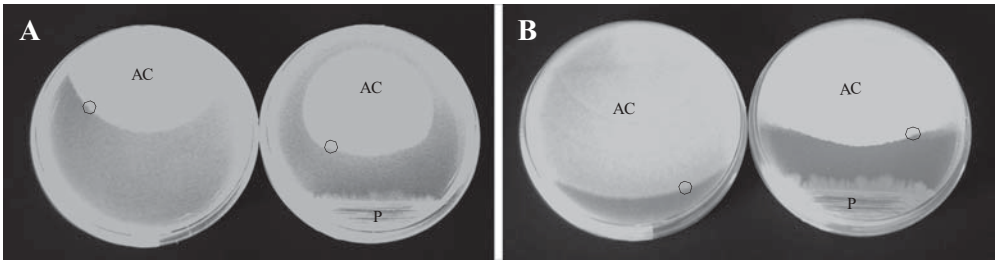

Fig. 1A,B. In vitro interactions between *Aphanomyces cochlioides* AC-5 and *Pseudomonas* sp. strain EC-S101 on potato dextrose agar (PDA) medium at day 3 and day 5. **A** AC-5 grown in single culture (untreated control) and AC-5 grown in the presence of EC-S101 at day 3. Growth of AC-5 was slow and an inhibition zone of about 1.5 cm developed in the presence of EC-S101. **B** AC-5 in single culture and AC-5 in the presence of EC-S101 at day 5. Inhibition zone was nearly similar to that at day 3; radial growth of AC-5 hyphae growing toward EC-S101 appeared to be restricted after day 3. *Circled areas* indicate part of agar plugs harvested with a sterile cork borer (6 mm i.d.) for confocal laser scanning and transmission electron microscopic study of growing hyphae. *AC*, *Aphanomyces cochlioides* AC-5; *P*, *Pseudomonas* sp. EC-S101

CMA and PDA plates with only AC-5 for CLSM and TEM visualization, respectively.

CLSM specimen preparation and observation

The following stains were selected in order to observe the physiological changes evoked in the hyphae: Nile red (Sigma N-3013, Steinheim, Germany) for lipid bodies; 3,3′-diheptyloxacarbocyanine iodide ($DIOC_7$) (Molecular Probes D-378, Eugene, OR, USA) for mitochondria and Hoechst 33258 (bisbenzimide) (Sigma-Aldrich H 6024, St. Louis, MO, USA) for visualization of nuclei. Stock solutions of the stains were made at 1 mg/ml in dimethylsulfoxide (DMSO) except for Hoechst 33258. The final working concentrations and staining times were as follows: Nile red at 2 µl/ml for 20 min and $DIOC_7$ at 0.02 µl/ml for 60 min (Thrane et al. 1999). Hoechst 33258 was used at 20 µg/ml ultrapure MilliQ (Millipore, Molsheim, France) water for 5 min.

Agar discs of AC-5 hyphae in dual culture with EC-S101 bacterial colonies and of the untreated control were harvested with a sterile cork borer (6 mm i.d.) and dipped in the staining solutions in a 24-well Nunc Petri dish (Nalge Nunc International, Roskilde, Denmark). After the agar discs were stained in the respective reagents, they were transferred to a glass slide for sectioning and subsequent visualization, and the top of the mycelial plug was sectioned uniformly (0.25 mm thickness) with a feather blade. The sections were then stained with Hoechst 33258 on the slide, then mounted in 50% glycerol solution in ultrapure MilliQ water and covered with a glass slip (0.12 mm thickness). Five mycelial disks from each of five replicate plates of the treated and negative control were sampled. An average of five hyphae were examined in each specimen.

The sections with stained hyphae were observed with a Zeiss confocal laser scanning microscope LSM410 (Carl Zeiss, Oberkochen, Germany) in order to detect the various fluorescence signals. The instrument was equipped with an Axiovert 135 M microscope with objective lenses containing magnifications/numerical apertures of 20/0.5 and 40/0.75. For Nile red and $DIOC_7$, an excitation wavelength of Ar488 nm and LP515 nm emission filter were used, and for Hoechst 33258, an excitation of UV-Ar364 nm and emission filter BP395–440 nm. Ar488 was used in order to mediate observations with differential interference contrast (DIC) microscopy. For fluorescence microscopy, images were sequentially collected from single optical sections along the z-axis at intervals of 1–1.5 µm. Approximately 10–30 optical sections were obtained from a total depth of optical sectioning of 1 µm. Randomly selected regions of specimens were scanned to compile images using the z-series program for CLSM. The optical sections were reconstructed into stereoscopic images with the CLSM reconstruction program. Images were processed by adding the following pseudocolors with Adobe Photoshop v.6.0.1: green for Nile red and $DIOC_7$, and blue for Hoechst 33258, to detect lipid bodies, mitochondrial localization and activity, and behavior of nuclei, respectively. However, only a single optical section was obtained for DIC images.

TEM specimen preparation and observation

Agar discs of AC-5 hyphae treated with bacterial colonies and the untreated controls were fixed with 2% glutaraldehyde (TAAB, Birkshire, UK) in sodium phosphate buffer (SPB) (10 mM, pH 7.2) for 3–6 h at 4°C. The samples were then thoroughly rinsed with phosphate buffer (SPB) (8 mM; pH 7.2) for 3 h, postfixed with osmium tetroxide (10 g/l) in SPB for 2 h at 4°C and rinsed with buffer. Samples were then dehydrated in a graded acetone series (50%, 70%, 90%, and 99.5%), embedded with Epon 812 (electron microscopy grade; TAAB) and polymerized at 60°C for 24 h. Ultrathin sections (100 nm thickness) were cut with a diamond knife (SK1045, Sumitomo, Tokyo) and stained with 2% uranyl acetate (5 min). Samples were washed with SPB, and sections were briefly stained with lead citrate (3 min). After staining, the sections were observed with a Hitachi H-800 TEM with an accelerating voltage of 75 kV. Four specimens were examined both for affected as well as untreated control hyphae.

Scanning electron microscope (SEM) specimen preparation and observation

To test the colonization ability of *Pseudomonas* sp. strain EC-S101 on the host roots, surface-sterilized seeds of spinach were coated with EC-S101 and allowed to germinate on 1/5 Hoagland's S medium solidified with 0.3% gellan gum as described (Islam et al. 2005). A 1-month-old seedling was prepared for SEM for studying the colonization of *Pseudomonas* sp. EC-S101 to the spinach roots as described earlier (Islam et al. 2005).

Oosporogenesis of *Aphanomyces cochlioides* AC-5 in the presence of *Pseudomonas* sp. strain EC-S101

Different populations of EC-S101 were suspended in a semisolid medium (5 g/l CMA and 1 g/l mycological peptone) that was designed by Paternoster and Burns (1996) to produce viable oospores. Sublethal doses of EC-S101 were added to the media at: 50, 150, 300, or 450 CFU/ml, then an AC-5 mycelial block was added to the center of a petri dish (9 cm i.d.). Five replicates were performed for both the treated hyphae and untreated controls. The oospores formed in the mycelial colony were counted with a light microscope (×500, IX70-S1F2, Olympus, Tokyo, Japan) in five different views of 0.27 mm^2 per dish.

Results

Pseudomonas sp. induces excessive branching in *Aphanomyces cochlioides* hyphae

Radial growth of *Aphanomyces cochlioides* AC-5 hyphae growing toward *Pseudomonas* sp. strain EC-S101 in the dual culture assay was relatively slower compared with that

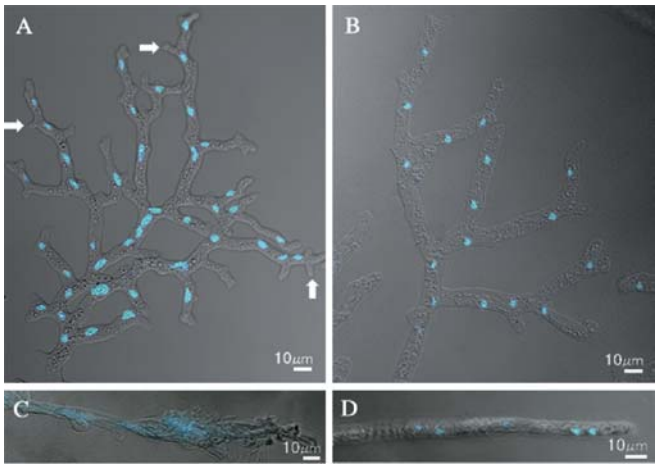

Fig. 2A–D. Hyphae of *Aphanomyces cochlioides* AC-5 stained with Hoechst 33258 to visualize nuclei at different stages of interaction with *Pseudomonas* sp. EC-S101 on corn meal agar (CMA) medium. **A**–**C** Induction of excessive branching (*arrows*, typical newly branching nodes) in AC-5 hyphae after interaction with EC-S101. **A** Hyphae showed an increase in the number of nuclei per unit length of the hyphae with no change in shape (oval) during early stage at day 3. **B** Nuclei became spherical during advanced stage at day 3. **C** Collapsed hyphae. Prolonged exposure (7 days) of EC-S101 to AC-5 induced disintegration of nuclei and release of nuclear material in the disorganized cytoplasm of AC-5. **D** Untreated hyphae. The oval nuclei are few in number. Filter set (Hoechst 33258): excitation, UV-Ar364 nm; emission, BP395–440 nm

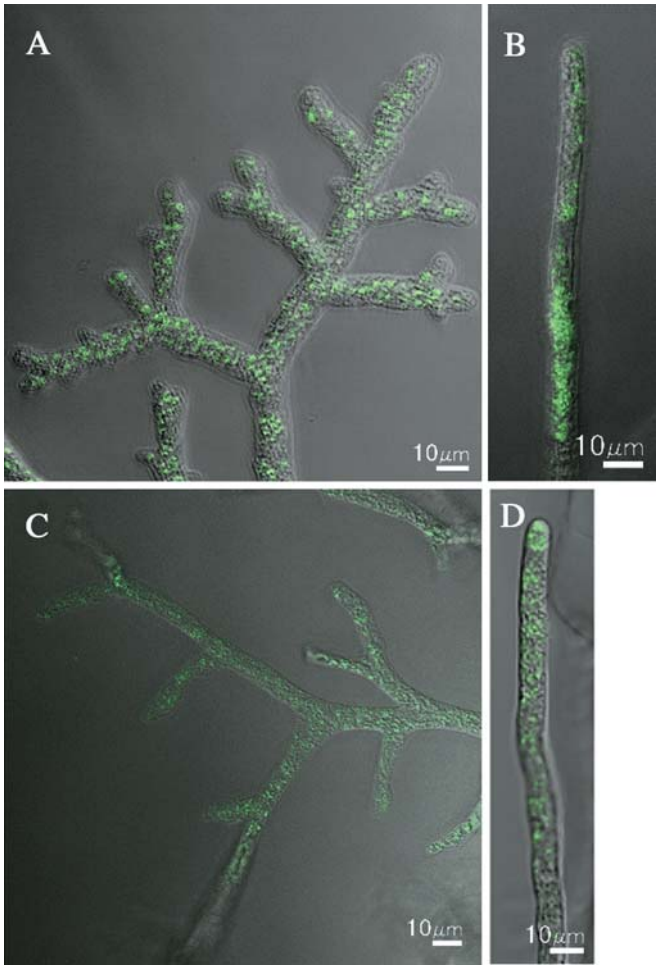

Fig. 3A–D. Hyphae of *Aphanomyces cochlioides* AC-5 stained with Nile red and $DIOC_7$ to visualize lipid bodies and mitochondria, respectively, during interaction with *Pseudomonas* sp. EC-S101 on CMA medium. **A** Induction of excessive branching in AC-5 hyphae. Increase in number and size of lipid bodies with globular shapes and their uniform distribution throughout the affected mycelium are seen during the early stage at day 3 of interaction. **B** Untreated hyphae. Fewer lipid bodies and of variable sizes are distributed randomly. **C** A reduced intensity of fluorescence depicted a decrease in the number of mitochondria throughout the affected mycelia during the advanced stage of day 3 of interaction, lower than that of the high fluorescent intensity in the untreated control hyphae (**D**). Filter set (Nile red and $DIOC_7$): excitation, Ar488 nm; emission, LP515 nm

without EC-S101. At day 3, radial growth of AC-5 hyphae growing toward EC-S101 appeared to be restricted; an inhibition zone had developed between the organisms (Fig. 1A). The inhibition zone remained constant after day 3. Figure 1B shows the inhibition at day 5 on PDA. However, the inhibition zone on PDA was larger (about 15 mm) than that on CMA (about 10 mm) at day 3 of interaction. In the presence of EC-S101, AC-5 hyphae growing toward bacterial colonies displayed a remarkable increase in branching frequency by apical bifurcation (Fig. 2A) as compared with that of untreated control (Fig. 2D). This excessive branching induction in AC-5 hyphae was initiated on day 1 of interaction with EC-S101. Because replicates of the hyphal samples growing toward the bacterial colonies were harvested randomly from different places for CLSM and TEM studies, two different stages of interactions were observed depending on the hyphal condition (Fig. 2A, B): the early stage of interaction (less affected hyphae, Fig. 2A), when hyphae had a radial growth, and a more advanced stage of interaction (severely affected hyphae, Fig. 2B), having a little or no radial growth.

Pseudomonas sp. affects nuclei, lipid bodies, and mitochondria in *Aphanomyces cochlioides*

By using Hoechst 33258 to visualize division and location of nuclei, we noted a decrease in the distance between two successive nuclei in the excessively branched hyphae compared with the untreated control hyphae of AC-5. On average (n = 10), the distance between two successive nuclei in the untreated control hyphae was ca. 42 µm (ranging 10–60 µm) as compared with ca. 19 µm (ranging 10–50 µm) in the affected hyphae. This difference in distance was probably due not only to excessive branching, but also due to the hyphal swelling induced by strain EC-S101. The mean diameter of the matured affected hyphae (n = 10) was ca. 10 µm (Fig. 2A) compared with ca. 7 µm (Fig. 2D) of mature, untreated control hyphae, a twofold increase in volume. At this stage, the shape (oval shaped) of the nuclei in the treated hyphae did not differ from the untreated control hyphae (Fig. 2A, D).

Moreover, branch formation in the affected hyphae was coordinated with the nuclear division. From ten observations, we found that each branch corresponded to one or a fraction more than one nucleus. For instance, the number of branches and number of nuclei in Fig. 2A (early stage) and Fig. 2B (advanced stage) are 42 and 42, and 17 and 15, respectively. At the more advanced stage of interaction at day 3, all nuclei were now round (Fig. 2B). Finally, after a prolonged interaction (7 days), the nuclei had disintegrated (Fig. 2C). The dispersion of the fluorescence signals throughout the hyphae depicted the release of nuclear material into the disorganized cytoplasm.

Nile red staining confirmed a fair increase in the number (1.4 times) and size (up to 1.5 times) of lipid bodies with globular shapes and variable sizes (ranging 0.5–1 μm) throughout the bacteria-exposed hyphae at day 3 (early stage of interaction, Fig. 3A) compared with the negative control (ranging 0.5–0.7 μm, Fig. 3B). This increase in the number of lipid bodies in the excessively branched hyphae indicated a general increase in the overall hydrophobicity of the cell. The number of lipid bodies remained high in the hyphae exposed to a more severe interaction during 3 days of cultivation, compared with those of untreated controls (data not shown).

In the excessively branched hyphae, mitochondria were significantly more abundant and evenly distributed throughout the main hyphae and its branches during early stage of interaction at day 3, in contrast to the untreated control with less densely distributed mitochondria (data not shown). However, the fluorescence intensity became relatively weak in the affected AC-5 hyphae (Fig. 3C) during a more advanced stage of interaction at day 3 in comparison with that of the control hyphae (Fig. 3D), indicating low respiratory activity in the affected hyphae compared with untreated control. Changes in mitochondrial shape were discerned with transmission electron microscopy.

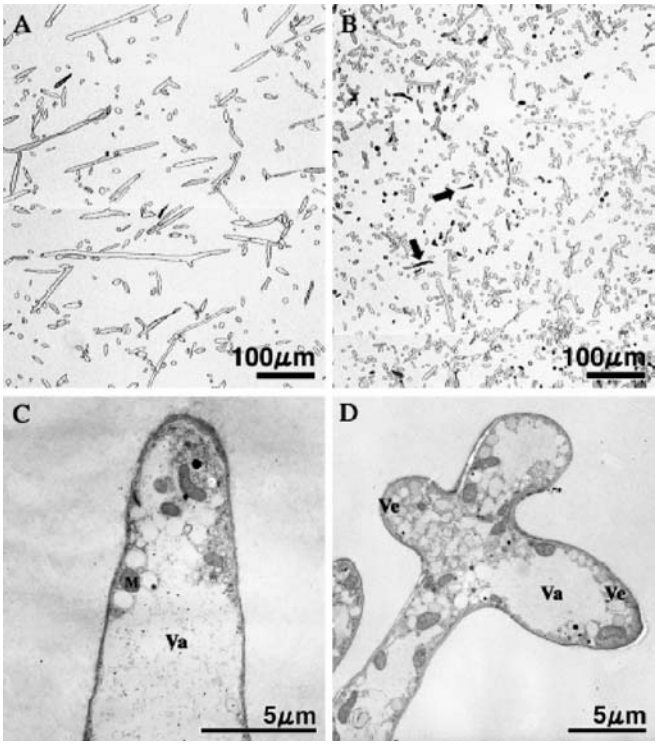

Fig. 4A–D. Light and transmission electron micrographs of *Aphanomyces cochlioides* AC-5 hyphae growing toward colonies of *Pseudomonas* sp. EC-S101 at day 5 of interaction on PDA medium. **A**, **B** TEM section viewed with a light microscope. **A** Hyphae with normal branching density and with no signs of necrosis. **B** High density of induced branching and necrotic hyphae (*arrows*). **C**, **D** Transmission electron micrographs of the longitudinal section. **C** Normal organization of cell organelles. **D** Increase in number of cell organelles with a mosaic distribution. *Va*, vacuole; *Ve*, vesicle; *M*, mitochondria

Pseudomonas sp. alters ultrastructure of *Aphanomyces cochlioides*

TEM sections of samples (viewed under normal microscope) starting at 5 days of interaction of the hyphae of AC-5 with EC-S101 revealed a high frequency of branching and necrosis (18%) in the hyphae growing toward the bacterial colony (Fig. 4B) in comparison with control (Fig. 4A). In a longitudinal section of treated hyphae, organelles were distributed in a mosaic pattern (Fig. 4D) in contrast to the uniform organization of the negative control (Fig. 4C). The number of vesicles and mitochondria greatly increased in the treated samples at an early stage of interaction, as opposed to the control hyphae. Vesicles mainly accumulated near the cell walls and in the growing tips. In transverse sections of treated hyphae, the cell walls were also thicker (Fig. 5B) than those of untreated control (Fig. 5A). In the treated hyphae, fibrous material had formed near vesicles and was presumed to be degenerated vesicles (Fig. 5B, arrow).

On the other hand, the lipid bodies became closely associated with the outside of the tonoplast membrane of the vacuole (Fig. 5C, arrow) and finally sank into the vacuolar lumen (Fig. 5D, arrow). In cross section (Fig. 5E), irregularities in hyphal diameter were common in the treated hyphae at an advanced stage of interaction when the nucleus disintegrated and the cytoplasm was disorganized (arrow). Severely affected hyphae growing toward bacterial colonies had an enlarged vacuole filled with an electron-dense material (Fig. 5F). In addition, cell wall invaginations (arrow) and changes in mitochondrial shape (arrowhead) were also visible (Fig. 5G). Furthermore, nonmembranous electron-transparent inclusion bodies were often irregularly distributed in the affected hyphae (Fig. 5G).

Pseudomonas sp. EC-S101 efficiently colonizes host roots

SEM observations of a 1-month-old root specimen from a seed preinoculated with EC-S101 and grown in 1/5 modified Hoagland's S medium solidified with 0.3% gellan gum, revealed that isolate EC-S101 colonized the spinach root surface extensively and formed very dense biomat (Fig. 6).

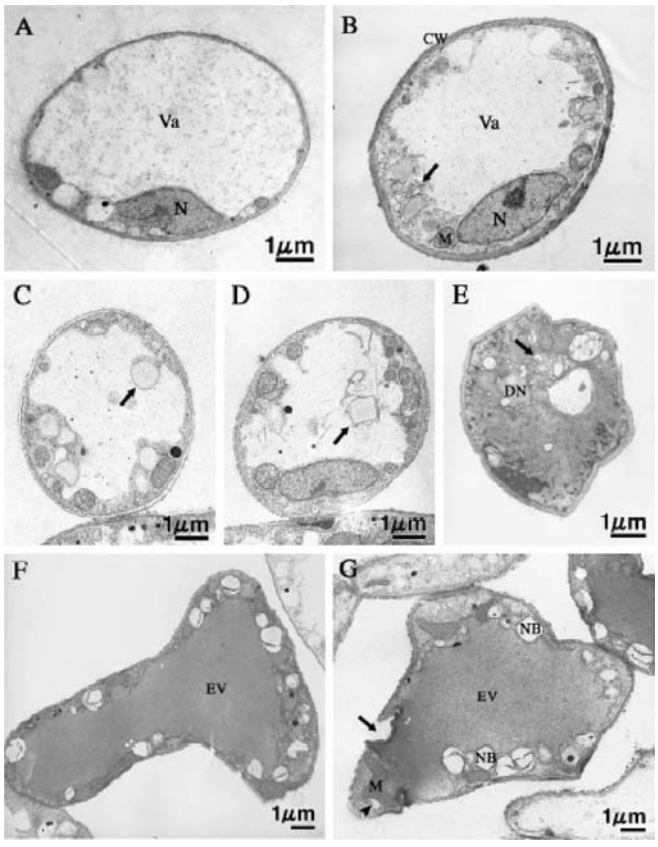

Fig. 5A–G. Transmission electron micrographs of *Aphanomyces cochlioides* AC-5 hyphae growing toward colonies of *Pseudomonas* sp. EC-S101 at day 5 of interaction grown on PDA medium. **A** Normal cell wall. **B** Thickened cell wall and degenerated vesicles (*arrow*). **C** Lipid bodies (*arrow*) become closely associated with the outside of the tonoplast membrane of the vacuole. **D** Lipid bodies have sunk into the vacuolar lumen. **E** Irregular shape of the cell with disintegrated nucleus and disorganized cytoplasm (*arrow*). **F** Vacuoles became enlarged and filled with electron-dense material. **G** Invagination of cell wall (*arrow*) took place after enlargement of vacuoles. Numerous nonmembranous electron-transparent inclusion bodies were also frequently observed. Shape of mitochondria is abnormal (*arrowhead*). *N*, nucleus; *Va*, vacuole; *Ve*, vesicle; *M*, mitochondria; *CW*, cell wall; *DN*, disintegrated nucleus; *EV*, electron-dense vacuole; *NB*, nonmembranous inclusion bodies

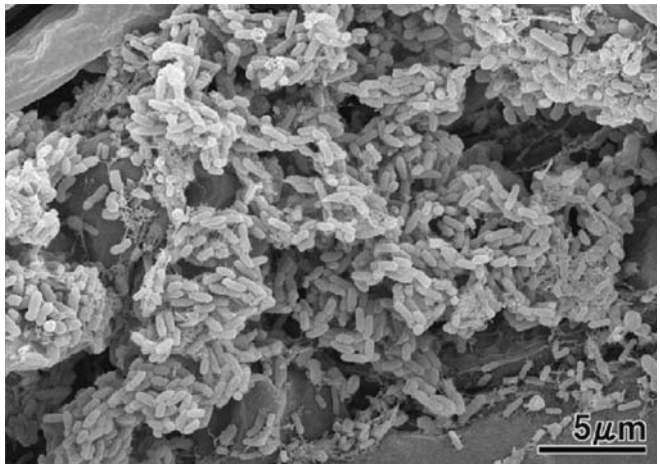

Fig. 6. High colonization of spinach root surface by *Pseudomonas* sp. EC-S101

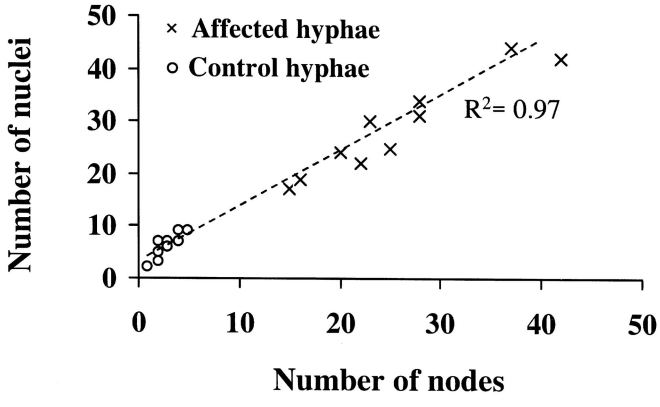

Fig. 7. Correlation between number of nuclei and number of nodes (branches) in affected and control hyphae of *Aphanomyces cochlioides* AC-5. The nuclei number and branch production are linearly correlated (r^2 = 0.97, slope = 1.01) in the control hyphae of *A. cochlioides* AC-5 and those encountering *Pseudomonas* sp. strain EC-S101. These observations indicate coordination of mitosis and branch production in Peronosporomycete hyphae. However, correlation between nuclei and branch production in the control hyphae shows a greater slope (r^2 = 0.73, slope = 1.73) than that of the affected hyphae (r^2 = 0.90, slope = 1.02), when the correlations were calculated separately. Among the control hyphae, correlation between numbers of nodes and nuclei is not reliable due to its lower values in these parameters than the affected hyphae. Hence, in an observed area under CLSM, correlation (*broken line*) for all plots of control and affected hyphae was used to compare the possible mitosis frequency replacing the numbers of node both in the affected and control hyphae

Discussion

In this study we used two different media, CMA and PDA, to observe the interactions between *Aphanomyces cochlioides* AC-5 hyphae and *Pseudomonas* sp. strain EC-S101 with CLSM and TEM, respectively. The physiological responses in the untreated control and affected AC-5 hyphae observed with CLSM were similar on CMA and PDA (data for CLSM study on PDA is not shown). The study of the day 5 interaction was specifically aimed toward understanding the physiology of the hyphae that appeared to be restricted in radial growth after day 3. Using TEM at this stage allowed us to study other phenomena such as cell wall thickness and invagination, vacuolar changes, mitochondrial shape, and nonmembranous electron-transparent inclusion bodies, in addition to those organelle responses targeted with CLSM.

A striking phenomenon observed in the AC-5 hyphae interacting with EC-S101 was the dynamics of the nuclear behavior in the hyphal cells. The diameter of the matured affected hyphae was found to be ca. 10 μm compared with ca. 7 μm of matured untreated control hyphae, which means a twofold increase in the volume, which decreased the successive distance between two nuclei in the affected hyphae

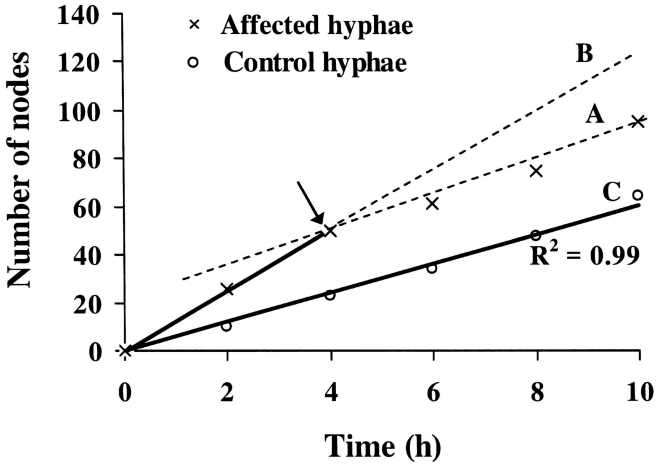

Fig. 8. Time course of increase in number of branches in *Aphanomyces cochlioides* AC-5 hyphae during interaction with *Pseudomonas* sp. EC-S101 in comparison with untreated control hyphae. The nodes were counted by visual observation (Deora et al. 2005). At any given time, the number of nodes was always higher in the treated hyphae (*lines A and B*) compared with control (*solid line C*). Control had a strong linear correlation between numbers of nodes and nuclei (*line C*, regression coefficient $R^2 = 0.99$), and its inclination coefficient was 6.1. On the other hand, it was difficult to count all the branching nodes in the affected hyphae, specifically those from the submerged hyphae. Therefore, after 4 h (*arrow*), *broken line A* with inclination coefficient 6.4 depicted the numbers of branching nodes visible from the upper side, which did not include the number of excessively branching nodes hidden in the submerged hyphae. Thus, a sudden decline in the curve was seen after 4 h and the rate of branch production become almost parallel to control hyphae. However, *broken line B* with inclination coefficient 11.5 suggests the real number of branches induced over time, i.e., almost double the number of nodes in the control hyphae, indicating acceleration in branch production along with mitosis in the affected AC-5 hyphae

(ca. 19 µm) to almost half that of the untreated control (ca. 42 µm). Therefore, the volume of the cytoplasm per nucleus appears to be almost similar both in affected hyphae (ca. 1490 µm^3/nucleus) and control hyphae (ca. 1615 µm^3/nucleus). Our results are supported by the fact that the number of nuclei is directly correlated to unit volume of cytoplasm and that hyphal diameter is the key determinant in hyphae for regulating the amount of branching (Dynesen and Nielsen 2003).

In an earlier time-course study, we demonstrated an increase in the numbers of nodes and nuclei in an excessively branched hypha of AC-5 (Deora et al. 2005) and compared this with the branches induced in an untreated control hypha in the present study (Fig. 7 and Fig. 8). At any given time, hyphae encountering EC-S101 had branched more than the control hyphae did (Fig. 8), thereby indicating acceleration in the induction of branching in the affected hyphae. Because branching is coordinated with mitosis (Dynesen and Nielsen 2003), acceleration in the induction of branching in AC-5 hyphae upon interaction with EC-S101 must also be associated with an acceleration in mitosis.

At a more advanced stage of interaction, the nuclei became round, which may have been due to the highly stressful condition exerted by the bacteria. Finally, after a prolonged interaction, the extranuclear staining by Hoechst 33258 in the cytoplasm of AC-5 hyphae suggested that the antagonistic effect of the bacterium EC-S101 damaged the nucleus, and led to a loss of control of normal cellular activities and subsequent cell death. Similar dynamics of nuclear behavior were found in *Pythium ultimum* hyphae after exposure to viscosinamide, a compound produced by *Pseudomonas fluorescens* DR54 (Thrane et al. 1999).

In a dual culture assay with EC-S101 impregnated in the solid medium, excessively branched AC-5 mycelia (2n) produced neither oogonia nor antheridia, unlike that of control mycelia that produced abundant oospores (ca. 50 per 0.27 mm^2). Hence, EC-S101 likely hinders the progression of the normal cell cycles leading to a loss of the sexual stage in AC-5. This loss is an important aspect of the antagonism because the pathogen might become unable to acquire genotypic resistance against the antagonistic rhizobacteria.

In addition, in TEM observations at an advanced stage at day 5, most of the AC-5 hyphal lumen was occupied by the enlarged vacuoles, into which the lipid bodies had sunk. Similar extensive vacuolation was observed in the hyphae of the root rot pathogen, *Fusarium oxysporum* f. sp. *radicis-lycopersici*, in the tomato rhizosphere after inoculation with biocontrol agent *Pseudomonas chlororaphis* PCL1391, suggesting that the aging of the fungus is accelerated, possibly reducing its aggressiveness toward its host (Bolwerk et al. 2003). We previously demonstrated the in vivo suppression in damping-off mediated by AC-5 (Deora et al. 2005). It is therefore suggested that the extensive vacuolation and sinking of lipid bodies might have contributed to the suppression of AC-5 and disease mediated by it. Because vacuoles play a role in degradation of redundant organelles (Weber 2002), the electron density of the vacuole in AC-5 hyphae (Fig. 5F, G) could be due to the degradation of redundant lipids. Such an illustration of lipids being degrading by sinking into the vacuoles of the hyphal cells of a plant pathogen under the stressful conditions evoked by an antagonistic bacterium is unprecedented.

Based on this discussion, *Pseudomonas* sp. EC-S101 apparently inhibits the in vitro radial growth of AC-5 hyphae. This in vitro growth inhibition is likely to have the same mechanism as the suppression of damping-off caused by AC-5 in spinach and sugar beet under in vivo conditions shown in our previous study (Deora et al. 2005). Our results are supported by a report on strain DR54 of *P. fluorescens* (Thrane et al. 1999) that also induced excessive branching in some of the Peronosporomycetes and fungal hyphae due to the production of antimicrobial compound viscosinamide. Furthermore, bacterial cells of *P. chlororaphis* PCL1391 and its secondary metabolite, phenazine-1-carboximide, also induced similar excessive branching in fungal hyphae (Bolwerk et al. 2003).

This is the first report that a gram-negative rhizobacterium, '*Pseudomonas jessenii* EC-S101', efficiently suppresses a root-associating pathogen and can colonize plant roots. From our observations, the excessive branching pattern in AC-5 induced by EC-S101 resulted through apical bifurcation of the successive hyphae (Fig. 2A). In

contrast, viscosinamide and phenazine-1-carboxamide induced excessive branching in other fungal and Peronosporomycete hyphae by the production of more lateral branches. Nonetheless, the induction of excessive branching in AC-5 involved secondary metabolites, because methanol-soluble extracts from the culture fluids of *Pseudomonas* sp. EC-S101 induced excessive branching in the AC-5 hyphae similar to that induced by interaction with colonies of EC-S101 (Deora et al. 2005). However, the secondary metabolite(s) produced by *Pseudomonas* sp. EC-S101 is likely to be an unknown compound(s).

We, therefore, conclude that the in vitro intercellular interaction between *Pseudomonas* sp. strain EC-S101 and *A. cochlioides* AC-5 is a multifaceted process, which might be mediated by an extensive disturbance of biologically active principle(s). The complex responses evoked, lead to a series of intracellular events and ultimately to death of the pathogen. Bioassays are currently underway to explore the nature of the secondary metabolites that induce these morphophysiological abnormalities. Our approach to understanding the morphophysiological responses of Peronosporomycete toward antagonistic bacterium promises to aid the development of a better disease management program.

Acknowledgments We thank Dr. R.K. Behl, CCS Haryana Agricultural University, India, for discussions and review of the manuscript. Financial support from Grants-in-Aid for Scientific Research (no. 16208032 to Y.H. and no. 14206013 to S.T.) and a scholarship for the first author at Hokkaido University from the Ministry of Education, Culture, Sports, Science, and Technology, Japan (MEXT), are gratefully acknowledged.

References

Benhamou N, Rey P, Picard K, Tirilly Y (1999) Ultrastructural and cytochemical aspects of the interaction between the mycoparasite *Pythium oligandrum* and soilborne plant pathogens. Phytopathology 89:506–517

Bolwerk A, Lagopodi AL, Wijfjes AHM, Lamers GEM, Chin-A-Woeng TFC, Lugtenberg BJJ, Bloemberg GV (2003) Interactions in the tomato rhizosphere of two *Pseudomonas* biocontrol strains with the phytopathogenic fungus *Fusarium oxysporum* f. sp. *radicis-lycopersici*. Mol Plant-Microbe Interact 16:983–993

Deora A, Hashidoko Y, Islam MT, Tahara S (2005) Antagonistic rhizoplane bacteria induce diverse morphological alterations in Peronosporomycete hyphae during in vitro interaction. Eur J Plant Pathol 112:311–322

Dunne C, Moënne-Loccoz Y, McCarthy J, Higgins P, Powell J, Dowling DN, O'Gara F (1998) Combining proteolytic and phloroglucinol-producing bacteria for improved biocontrol of *Pythium*-mediated damping-off of sugar beet. Plant Pathol 47:299–307

Dynesen J, Nielsen J (2003) Branching is coordinated with mitosis in growing hyphae of *Aspergillus nidulans*. Fungal Genet Biol 40:15–24

Hansen M, Thrane C, Olsson S, Sørensen J (2000) Confocal imaging of living fungal hyphae challenged with the fungal antagonist viscosinamide. Mycologia 92:216–221

Hogan DA, Kolter R (2002) *Pseudomonas–Candida* interactions: an ecological role for virulence factors. Science 296:2229–2232

Homma Y, Uchino H, Kanzawa K, Nakayama T, Sayama M (1993) Suppression of sugar beet damping-off and production of antagonistic substances by strains of rhizobacteria. Ann Phytopathol Soc Jpn 59:282 (abstract in Japanese)

Huang Z, Bonsall RF, Mavrodi DV, Weller DM, Thomashow LS (2004) Transformation of *Pseudomonas fluorescens* with genes for biosynthesis of phenazine-1-carboxylic acid improves biocontrol of rhizoctonia root rot and in situ antibiotic production. FEMS Microbiol Ecol 49:243–251

Islam MT, Hashidoko Y, Deora A, Ito T, Tahara S (2005) Suppression of damping-off disease in host plants by the rhizoplane bacterium *Lysobacter* sp. strain SB-K88 is linked to plant colonization and antibiosis against soilborne Peronosporomycetes. Appl Environ Microbiol 71:3786–3796

Kang Z, Huang L, Krieg U, Mauler-Machnik A, Buchenauer H (2001) Effects of tebunconazole on morphology, structure, cell wall components and trichothecene production of *Fusarium culmorum* in vitro. Pest Manag Sci 57:491–500

Nakayama T, Homma Y, Hashidoko Y, Mizutani J, Tahara S (1999) Possible role of xanthobaccins produced by *Stenotrophomonas* sp. strain SB-K88 in suppression of sugar beet damping-off disease. Appl Environ Microbiol 65:4334–4339

Paternoster MP, Burns RG (1996) A novel medium for the oosporogenesis of *Aphanomyces cochlioides*. Mycol Res 100:936–938

Savchuk S, Fernando WGD (2004) Effect of timing of application and population dynamics on the degree of biological control of *Sclerotinia sclerotiorum* by bacterial antagonists. FEMS Microbiol Ecol 49:379–388

Thrane C, Olsson S, Nielsen TH, Sørensen J (1999) Vital fluorescent stains for detection of stress in *Pythium ultimum* and *Rhizoctonia solani* challenged with viscosinamide from *Pseudomonas fluorescens* DR54. FEMS Microbiol Ecol 30:11–23

Weber RWS (2002) Vacuoles and the fungal lifestyle. Mycologist 16:10–20

Whipps JM (2001) Microbial interactions and biocontrol in the rhizosphere. J Exp Bot 52:487–511

Williams GE, Asher MJC (1996) Selection of rhizobacteria for the control of *Pythium ultimum* and *Aphanomyces cochlioides* on sugarbeet seedlings. Crop Prot 15:479–486